

Design of optimal trajectory transition controller for thrust-vectorred V/STOL aircraft

Zhiqiang CHENG^{1,2}, Jihong ZHU^{1*}, Xiaming YUAN¹ & Xiangyang WANG¹

¹Department of Computer Science and Technology, Tsinghua University, Beijing 100084, China;

²Key Laboratory of Complex Ship System Simulation, Beijing 100161, China

Received 28 June 2018/Accepted 3 August 2018/Published online 14 April 2020

Citation Cheng Z Q, Zhu J H, Yuan X M, et al. Design of optimal trajectory transition controller for thrust-vectorred V/STOL aircraft. Sci China Inf Sci, 2021, 64(3): 139201, https://doi.org/10.1007/s11432-018-9582-6

Dear editor,

In recent years, vertical and/or short take-off and landing (V/STOL) aircraft have attracted much attention because they combine the efficiency of fixed-wing vehicles with the flexibility of traditional vertical take-off and landing aircraft, such as a helicopter. Thrust-vectorred V/STOL is often used for fighter jets (e.g., F-35B). However, the design of an autonomous transition controller for thrust-vectorred V/STOL is challenging because of the nonlinearity and strong coupling in the transition process [1]. In this study, the transition process refers to transiting from hover state to wing-borne flight or vice versa.

Many studies on controller design for V/STOL autonomous transition have been conducted, and most were based on tilt-wing or tail-sitter aircraft. Although thrust-vectorred V/STOL aircraft share many similarities with other V/STOL aircraft, their own unique characteristics should be considered. For tilt-wing aircraft, the bandwidth of the tilt angle is much lower than that of the propeller when the moment of inertia of the aircraft wing is large. Therefore, the tilt angle does not participate in attitude control, which is affected by the propeller. Therefore, the tilt angle is adjusted based on velocity until it reaches 0°, and the attitude is controlled by a linear gain-scheduled controller [2]. For thrust-vectorred V/STOL aircraft, the bandwidth of the main turbojet engine is much lower than that of the three bearing swivel duct (3BSD) or lift fan, which are involved in altitude control, achieving good transition performance. Because the angle of the 3BSD and lift fan results in nonlinear control force for attitude and velocity, the mode of the tilt-wing aircraft controller cannot be applied. Furthermore, three variables (i.e., velocity, 3BSD nozzle, and angle of lift fan) cause nonlinearity in thrust-vectorred V/STOL aircraft. Therefore, most transition controllers for tilt-wing or tail-sitter aircraft are not applied directly, except when locking the angle of the lift fan. In [3], a transition controller was designed with a fixed angle of the lift fan. However, this clearly deteriorated performance.

This study proposes an optimal trajectory transition con-

troller. The main idea is designing an optimal transition trajectory and a feedback controller to keep the flight states near the appropriate trajectory during transition. To get the numerical solution of optimal transition trajectory, direct optimization is employed (i.e., Cauchy method or steepest descent). However, the gradients computed by the Cauchy method [4, 5] are not sufficiently accurate, causing the optimization to require a long time. To overcome this shortcoming, a new optimizing method is proposed, which uses backward propagation to compute gradient. Based on optimal trajectory, a new transition controller is designed.

Optimization technique. Our longitudinal dynamic model of thrust-vectorred V/STOL is the same as [6]. Considering actuator dynamics, all dynamics can be represented as follows:

$$\dot{x} = f(x) + Bu_c, \quad \text{s.t. } p_l \leq u_c \leq p_h, \quad (1)$$

where $f(x)$ and B represent the vehicle dynamics and actuator dynamics, and p_l and p_h are the position limits vector of actuators. To deal with state and control constraints, the extended cost function can be shown as follows:

$$J = \phi(x(t_f), t_f) + \int_0^{t_f} L(x, u) + \rho \sum c_i(t) dt, \quad (2)$$

where ϕ penalizes the final state and L penalizes the state and controller input during the control process. c_i is the state and control variable inequality constraint. To get the optimal trajectory, the period is discretized into N segments, and the matrix $U_c = [u_c(t_0) \cdots u_c(t_{N-1})]$ and t_f is the optimization parameters. To minimize the cost function J in (2), the derivatives $\frac{\partial J}{\partial U_c}$ and $\frac{\partial J}{\partial t_f}$ should be computed. Because we can convert a minimum time into fixed-end time as [5] does, the sample time should be $T = 1/N$. We use $h(x) = t_f \times f(x)$ and $B^* = t_f \times B$ to represent the new dynamics. According to the Fourth-order Runge-Kutta integration algorithm, $x(t_{k+1})$ can be calculated as follows:

$$K_1 = h(x(t_k)) + B^* u_c(t_k),$$

$$K_2 = h\left(x(t_k) + \frac{T}{2} \times K_1\right) + B^* u_c(t_k),$$

* Corresponding author (email: jhzhu@tsinghua.edu.cn)

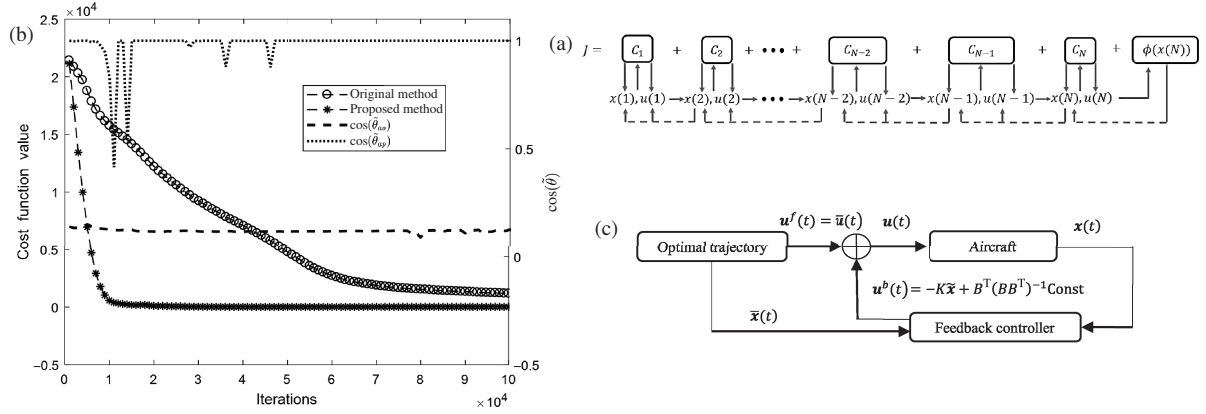


Figure 1 (a) Computation process of the proposed method; (b) cost function values and cosine values of the original and proposed methods; (c) optimal trajectory controller structure.

$$\begin{aligned} K_3 &= h \left(x(t_k) + \frac{T}{2} \times K_2 \right) + B^* u_c(t_k), \\ K_4 &= h(x(t_k) + T \times K_3) + B^* u_c(t_k), \\ x(t_{k+1}) &= x(t_k) + \frac{T}{6} (K_1 + 2K_2 + 2K_3 + K_4), \end{aligned} \quad (3)$$

where K_1 , K_2 , K_3 , and K_4 are the median values. Based on (3), derivatives of $\partial x(t_{k+1})/\partial x(t_k)$ can be computed as follows:

$$\frac{\partial x(t_{k+1})}{\partial x(t_k)} = E + \frac{T}{6} \left(\sum_{i=1}^4 \frac{\partial K_i}{\partial x(t_k)} \right), \quad (4)$$

where E is the identity matrix. To simplify (2), we take

$$L(t_k) = L(x(t_k), u(t_k), t_k), \quad C(t_k) = \rho \sum_{i=1}^{c_n} c_i(t_k), \quad (5)$$

where $L(t_k)$ and $C(t_k)$ represent penalization based on the k th sample point. If we apply Euler's integration algorithm into (2), the cost function can be written as

$$J = \phi(x(t_f), t_f) + \sum_{k=0}^{N-1} (L(t_k) + C(t_k)) \times T. \quad (6)$$

The standard Fourth-order Runge-Kutta integration algorithm can also be applied here. To simplify our expression, the Euler integration is used. To get the minimum value of J in (6), the partial derivatives should be calculated using

$$\partial J / \partial U_c = \left[\partial J / \partial u_c(t_0) \quad \dots \quad \partial J / \partial u_c(t_{N-1}) \right]. \quad (7)$$

Because $u_c(t_i)$ for any t_i can only influence the state after t_i , the calculation of $\partial J / \partial u_c(t_i)$ can be simplified. Let $J(n)$ represent the costs produced after time t_n , which can be calculated by

$$J(n) = \phi(x(t_f), t_f) + \sum_{k=n}^{N-1} (L(t_k) + C(t_k)) \times T. \quad (8)$$

Therefore, it is easy to calculate $\partial J / \partial u_c(t_i) = \partial J(i) / \partial u_c(t_i)$ which can be further calculated as follows:

$$\begin{aligned} \frac{\partial J(i)}{\partial x(t_i)} &= \frac{\partial (L(t_i) + C(t_i)) \times T}{\partial x(t_i)} \\ &\quad + \frac{\partial J(i+1)}{\partial x(t_{i+1})} \frac{\partial x(t_{i+1})}{\partial x(t_i)}, \\ \frac{\partial J}{\partial u_c(t_i)} &= \frac{\partial J(i)}{\partial u_c(t_i)} \\ &= \frac{\partial (L(t_i) + C(t_i)) \times T}{u_c(t_i)} + \frac{\partial J(i+1)}{\partial u_c(t_i)}. \end{aligned} \quad (9)$$

The derivatives $\partial J(i) / \partial u_c(t_i)$ can be computed iteratively from $N-1$ to 0. The method of computing the derivative for t_f is same. The total computational process of the proposed method is shown in Figure 1(a). The dashed line indicates a derivative's feedback computation, whereas the solid line indicates forward computation.

To show the accuracy of both methods, the gradient-checking algorithm is applied. This algorithm computes derivatives using

$$\frac{\partial J(u_c(k))}{\partial u_c(k)} = \frac{J(u_c(k) + \varepsilon) - J(u_c(k) - \varepsilon)}{2\varepsilon}, \quad (10)$$

where ε equals 10^{-6} . To compare accuracy, we take the derivative dJ_a , computed by (10), as the anchor. We use dJ_p and dJ_o to represent the derivatives computed by the proposed and original methods separately. Their intersection angles with dJ_a are recorded as $\hat{\theta}_{ap}$ and $\hat{\theta}_{ao}$. Here, we do not use the Euclidean distance to measure accuracy because the direction is more important for derivatives. When the intersection angles $\hat{\theta}_{ap}$ or $\hat{\theta}_{ao}$ are small, their cosine values are near 1. Taking the hover-to-cruise transition as an example, the cost function value and the cosine value of the intersection value are shown in Figure 1(b).

Controller design. Traditionally, a controller is designed based on several trim points along a trajectory. Because the points along an optimal trajectory are not trim, we propose a new method here to make use of optimal trajectory.

Because it is obvious that an open-loop control cannot deal with the transition process well, feedback should be added to the controller. For (1), it is easy to use Taylor expansion at point (\bar{x}, \bar{u}) to get

$$\begin{aligned} \dot{x} &= f(x) + Bu \\ &= f(\bar{x}) + B\bar{u} + f'(\bar{x})(x - \bar{x}) + B(u - \bar{u}). \end{aligned} \quad (11)$$

If the point (\bar{x}, \bar{u}) is a trimmed point, $\text{Const} = f(\bar{x}) + B\bar{u}$ would be zero and LQR control method can be applied. For untrimmed points, the Const can be compensated by adding a constant value to u so that an LQR controller can still be used. Thus, u can be solved by

$$u = -K\bar{x} + \bar{u} + B^T(BB^T)^{-1}\text{Const}, \quad (12)$$

where K is computed by the LQR method and $\tilde{x} = x - \bar{x}$, $\tilde{u} = u - \bar{u}$. The last term is the compensation value for untrimmed points. Based on optimal trajectory and feedback controller, the control structure is shown in Figure 1(c). The controller selects the next point as the desired point, which is the closest to the real flight state. Then, the feedback controller computes the control value based on \tilde{x} .

Simulation. After optimization, the optimal t_f is 7.4 s for hover-to-cruise transition and 12.7 s for cruise-to-hover transition. In simulation, the gap between the optimal trajectory and the result of proposed method is very small. Compared with robust LPV proposed in [2], the transition process is quicker and steadier, which proves the efficiency of the proposed method.

Conclusion. An optimal trajectory transition controller for a thrust-vector V/STOL aircraft was developed in this study. The new optimizing method, which was developed to get the optimal trajectory, is faster. Based on optimal trajectory, a new transition method was developed to control the transition of the aircraft. This controller combined a gain-scheduled linear feedback controller and a feedforward compensation, which was easily solved. Compared to an LPV controller, our results showed that the transition response, based on the proposed method, is more stable and

faster.

Acknowledgements This work was supported by National Natural Science Foundation of China (Grant Nos. 61603210, 61673240).

References

- 1 Bordignon K, Bessolo J. Control allocation for the X-35B. In: Proceedings of Biennial International Powered Lift Conference and Exhibit, Virginia, 2002. 5–7
- 2 Dickeson J, Miles D, Cifdaloz O, et al. Robust LPV H-inf gain-scheduled hover-to-cruise conversion for a tilt-wing rotorcraft in the presence of CG variations. In: Proceedings of the 46th IEEE Conference on Decision and Control, Louisiana, 2007. 2773–2778
- 3 Xili Y, Yong F, Jihong Z. Transition flight control of two vertical/short takeoff and landing aircraft. J Guidance Control Dyn, 2008, 31: 371–385
- 4 Banazadeh A, Taymourtash N. Optimal control of an aerial tail sitter in transition flight phases. J Aircraft, 2016, 53: 914–921
- 5 Agrawal S, Fabien B. Optimization of dynamic systems. Kluwer Academic, 1999, 1: 103–106
- 6 Fan Y, Meng X Y, Yang X L, et al. Control allocation for a V/STOL aircraft based on robust fuzzy control. Sci China Inf Sci, 2011, 54: 1321–1326